Evaluation of Linear Fresnel Reflectors

Leonardo F. L. de Souza [1], Naum Fraidenraich [2], Chigueru Tiba [2] and Ikaro T. B. S. Barreto[2]

[1] Universidade Federal de Alagoas, Rio Largo, (Brasil)

[2] Universidade Federal de Pernambuco, Recife, (Brasil)

Abstract

We determine the thermal efficiency as a function of temperature for a large number of Linear Fresnel reflectors (LFRs) published in the literature, whose main geometrical and optical parameters are available. The thermal efficiency function combines properly the geometrical, optical and thermal properties of the LFR when those systems make part of a solar plant. The first part of the paper (Sections 2, 3 and 4) describes the methodology to obtain that function for the linear "aplanatic" Fresnel reflector, as well as the calculation of its annual energy absorbed for a region in the Brazilian Northeast. Results of the thermal efficiency function at normal incidence of various linear "aplanatic" Fresnel reflectors is presented showing that for DNI as high as 800 W/m², different LFARs tested can reach thermal efficiency between 59% and 77%. We also demonstrate that practical high-performance LAFR designs can achieve annual energy absorption efficiency as high as 61% at concentration values of 35. The second part (Section 6) synthetizes the thermal efficiency of the selected geometries at normal incidence. Results show that temperatures as high as 390 °C can be achieved with thermal efficiency between 60% and 75% for most part of geometries selected. A discussion is made about the choice of the probability function that governs the interval angle of light rays reaching the concentrator.

Keywords: Concentrating Solar Power, Fresnel Concentrator, Linear Fresnel, Solar Concentrator, Thermal Efficiency.

1. Introduction

Concentrating Solar Power (CSP) technology is highly versatile, supporting a wide range of applications. It uniquely offers thermal energy storage (TES), which is typically more cost-effective and durable than the battery storage used with photovoltaic (PV) generation. As a reliable, dispatchable renewable source, CSP integrates large-scale TES with synchronous machine characteristics, ensuring a stable and dependable connection to the power grid (Yao et al., 2024).

Beyond utility-scale, grid-connected power plants, CSP technologies show significant potential for various niche applications, including industrial process heat, water desalination, and the production of fuels and chemicals, as demonstrated in recent studies (Chen et al., 2018; Gude, 2018; Mishra and Singh, 2018; Souza et al., 2021). However, a paramount challenge for CSP deployment is the reduction of its Levelized Cost of Energy (LCOE). Achieving this cost reduction requires improvements across several areas, including the efficiency of the heat transfer fluid system, the storage system, component materials, and the overall efficiency of the solar collector field (Alami, 2023).

This present work focuses on the optical design evaluation of LFR concentrators based on their optical efficiency (η_{opt}), geometric concentration (C_g), and constructive characteristics favorable for reducing the LCOE. LFRs are specifically studied because they offer constructive advantages such as a stationary secondary reflector, single-axis tracking, and lower wind load on the mirror field (Giostri, 2012; Hussain and Lee, 2016). Nevertheless, without an innovative reflector design, these systems typically exhibit lower η_{opt} than Parabolic Trough Collectors (PTCs). PTCs currently account for 90% of the 6.8 peak GW of installed global CSP capacity (CSTA, 2022). PTCs typically achieve a geometric concentration of approximately 26 while maintaining an intercept factor above 0.9 (Manikandan et al., 2019). These performance metrics serve as the benchmark that new LFR designs incorporating a secondary concentrator aim to match.

Some studies present new LFR designs (Canavarro et al., 2014, 2017, Feuermann and Gordon, 1991, Hack et

10.18086/swc.2025.01.01 Available at http://proceedings.ises.org

al., 2017, Prasad et al., 2017, Qiu et al., 2017, Souza et al., 2023, Vouros et al., 2019, Zhu, 2013). However, most analyze the parameters of η_{opt} (measured at normal incidence) and C_g separately. To contribute to the optimization of LFR designs beyond those already discussed in the literature, this work presents a more thorough analysis using thermal efficiency curves as a function of absorber temperature and Direct Normal Irradiance (DNI), as well as a model to estimate the total absorbed energy considering double reflection. The efficiency curves are obtained using equations that combine η_{opt} and C_g in a single model, as shown in Section 4. A methodology for calculating the total annual energy absorbed by LFR concentrators that considers double reflection, locality, and available solar resource data is presented in Section 2.

Previous studies also do not discuss in depth the total distribution of errors used in each proposed project. These errors significantly influence the calculated η_{opt}, making it a limiting factor when comparing the performance between concentrators. An additional objective of this work is, therefore, to present an appropriate method for linear (two-dimensional) concentrators to normalize different probabilistic distributions of total errors, allowing a fair performance comparison between different LFRs if the geometry of each concentrator is known and can be included in a ray-tracing tool.

To comprehensively evaluate LFRs with secondary concentrators, ten devices published in specialized journals were selected based on publications that present new settings for double-reflection LFRs aimed at improving the optical effect publications that offer the necessary detail for the complete optical and thermal performance evaluation discussed in this work (presented in Section 5).

Specifically, this work aims to present: (a) A new model for estimating the absorbed energy, considering both double reflection on the secondary and direct reflection on the absorber. (b) An estimate of the annual energy absorbed by different linear aplanatic Fresnel concentrators using DNI data for Petrolina, Pernambuco, Brazil. (c) A calculation of the thermal efficiency curve of the selected LFR devices, considering the optical and thermal characteristics of the Schott absorber tube. (d) An evaluation of the influence of the mean squared value of the total probabilistic distribution of errors on the intercept factor.

2. Estimation model of annual energy absorbed

A model for annual absorbed solar energy estimation that considers double reflection was initially tested for a linear aplanatic Fresnel reflector, as complete geometric and ray-tracing information was available for this concentrator.

The efficiency of concentrating collectors can be defined by the Eq. 1, with the energy absorbed by the absorber (Q), the incident direct normal irradiance normal (DNI) at the aperture plane of the concentrator (I_b), expressed in W/m², the aperture area of the concentrator (A), in m² (Rabl, 1985):

$$\eta_{opt} = \frac{Q}{A.DNI.cos\,(\theta)} \qquad \text{(eq. 1)}$$

The optical efficiency uses the material properties of surfaces. ρ is the reflectivity of the primary and secondary mirrors, τ the transmissivity and α the absorptivity of the selective coating of the absorber tube and γ the total interception factor of the concentrator. Last, θ is the incidence angle at the aperture of the concentrator is the angle between the light beam that falls on the aperture and the normal to the aperture plane:

$$\eta_{opt} = \rho\tau\alpha\gamma(\theta) \qquad \text{(eq. 2)}$$

The angle, θ, can be decomposed into the transversal component (θ_t) and longitudinal component (θ_l) (McIntire, 1982), which define the orientation of the beams falling on the aperture of the concentrator, along the movement of the Sun, as shown in Fig. 1.

The η_{opt} varies with the position of the sun and can be calculated in function of θ components (McIntire, 1982; Zhu, 2013). In more realistic models, the optical properties are functions of θ. However, for simplicity in this analysis, the average values of these properties are considered (Howell et al., 2016).

$$\eta_{opt}(\theta_t, \theta_l) = \rho\tau\alpha\gamma(\theta_t, \theta_l) \qquad \text{(eq. 3)}$$

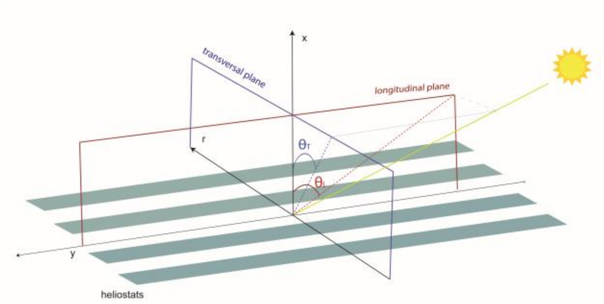

Figure 1. Transversal and Longitudinal incidence planes. Source: (Souza et al., 2023).

According to Bellos and Tzivanidis (2018), Gaul and Rabl (1980) and Santos et al. (2021) the efficiency curves of solar collectors are usually measured at normal incidence, which is the most suitable choice for standardized test conditions. However, the θ varies throughout the day and year. It can be considered when calculating the energy absorbed by linear concentrators, by modeling the total interception factor as the product of the partial interception factors in the eq. 4 where γ has been decomposed into the transverse and longitudinal component:

$$\gamma(\theta_t, \theta_l) \approx \gamma(\theta_t, 0)\gamma(0, \theta_l) \quad \text{(eq. 4)}$$

Utilizing this approximation, the measurements only need to be carried out with the incident angles throughout the North-South and East-West directions to properly specify the optical performance of the concentrator. The incident solar angle in the transverse and longitudinal direction are calculated using the solar incident angle (θ) and the solar azimuth (z) (Bellos and Tzivanidis, 2018; Wang et al., 2015):

$$\tan\theta_l = \cos z \tan\theta \quad \text{(eq. 5)}$$

$$\tan\theta_t = \sin z \tan\theta \quad \text{(eq. 6)}$$

The instantaneous energy absorbed can be obtained by the equation:

$$Q = \rho\tau\alpha.\gamma(\theta_t, 0).\gamma(0, \theta_l).A.I_b \quad \text{(eq. 7)}$$

Regarding the number of reflections and the reflectivity losses, it is considered that there is a fraction of rays that reach the absorber directly, making only one reflection. This fact is considered in the next section. For each incidence angle in the transverse and longitudinal planes there is a γ_1, referring to single reflection, and a γ_2, referring to dual reflection, being the total interception factor $\gamma = \gamma_1 + \gamma_2$ (Gomes et al., 2019). It is necessary to consider a value of ρ that represents the losses due to non-ideal reflections of the material for single and dual reflection. A weighted transverse ρ, in function of the transverse interception factors, γ_t, being $\gamma_t = \gamma_{1t} + \gamma_{2t}$. And the longitudinal weighted being $\gamma_l = \gamma_{1l} + \gamma_{2l}$.

$$\rho_t = \frac{\gamma_{1t}\rho + \gamma_{2t}\rho^2}{\gamma_t} \quad \text{(eq. 8)}$$

$$\rho_l = \frac{\gamma_{1l}\rho + \gamma_{2l}\rho^2}{\gamma_l} \quad \text{(eq. 9)}$$

Finally, the reflectivity becomes

$$\rho = \frac{(\gamma_t\rho_t + \gamma_l\rho_l)}{\gamma_t + \gamma_l} \quad \text{(eq. 10)}$$

and the optical efficiency can be obtained from the approximation:

$$\eta_o \approx \tau\alpha\gamma_t\gamma_l\frac{(\gamma_t\rho_t + \gamma_l\rho_l)}{\gamma_t + \gamma_l} \quad \text{(eq. 11)}$$

When the goal is to obtain a solar concentrator that maximizes the energy collection, in addition to time-varying op-tical efficiency, it is important to calculate the total energy absorbed in a certain period of time. This parameter depends on the optical properties of the concentrator, of the location and the solar resource available. The total energy absorbed by m² throughout the year, considering the hourly averages of the Ib, can be calculate by the following (Santos et al., 2021):

$$E_{year} \approx \tau\alpha \sum_{h=1}^{8760} \frac{(\gamma_t\rho_t+\gamma_l\rho_l)}{\gamma_t+\gamma_l} \gamma_t\gamma_l\, I_b \qquad \text{(eq. 12)}$$

3. Beam widths

As illustrated in Figure 2, the solar radiation cone reaching the concentrator's aperture can suffer unwanted angular deviations, which decrease the interception factor and, consequently, the optical efficiency.The effect of these errors can be evaluated using individual probabilistic distributions. However, the Central Limit Theorem (CLT) states that the convolution of a sufficiently large number of independent distributions approaches a Gaussian (normal) distribution, even if the individual errors are non-Gaussian. Therefore, it is often unnecessary to know the specifics of each individual probabilistic distribution; instead, the problem is reduced to finding their standard deviations (σ).

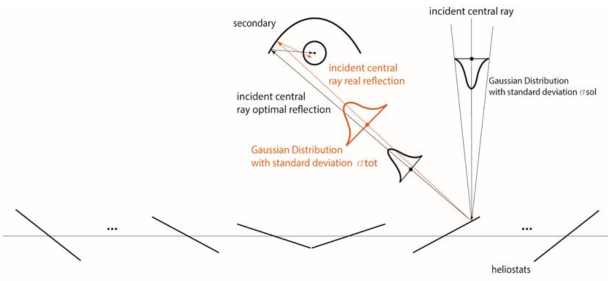

Figure 2. Total aperture of the linear Fresnel concentrator considering the gross area of the primary field, including the spaces between the mirrors.

For optical errors associated with solar concentrators, the individual distribution means are typically zero. Under this common condition (Fraidenraich and Lyra, 1995), the standard deviation of the resulting total error distribution (σ_{tot}), eq. 13, for a LFR in which σ_{sun}, σ_{mir}, σ_{geo}, σ_{geo}, σ_{abs} are, respectively, the standard deviations of the probabilistic distributions for: the sun's brightness (or shape), the specular reflection error, the geometric deformations of the reflective surfaces, the tracking error, and the absorber misalignment. The RMS value of σ_{tot} defines the total spreading of the radiation beam after reaching the CSP system.

$$\sigma_{tot} = \sqrt{\sigma_{sun}^2 + \sigma_{mir}^2 + (2\sigma_{geo})^2 + (2\sigma_{geo})^2 + \sigma_{abs}^2} \qquad \text{(eq. 13)}$$

The authors Abbas and Martínez-Val (2015), Biggs and Vittitoe (1979) and Pettit et al. (1983), assumed that errors due to the sun shape follow a uniform distribution, called “pill-box”, while the reflecting surfaces errors are Gaussian. The mean square width for a pill-box distribution, $\langle pb^2 \rangle$, depends on the half-angle of the impinging beam, θs, eq. 14. To make an analytical study pill-box and Gaussian are made equivalent, eq. 15.

$$\langle pb \rangle = \frac{\theta_s}{\sqrt{2}} \qquad \text{(eq. 14)}$$

$$\langle pb \rangle = \sqrt{2\sigma_{pb}^2} \qquad \text{(eq. 15)}$$

the dispersion of the equivalent Gaussian distributions results in:

$$\sigma_{pb} \approx \frac{\theta_s}{2} \qquad \text{(eq. 16)}$$

These considerations about the distributions and its parameters are important in order to compare different LFR, as shown in Section 5. This conversion was validate using Monte Carlo Ray Tracing simulation, with 1 milion rays. The authors presented a deduction for 3D concentrators, in which the heliostats track the sun in two axes (Central Tower). LFR are bidimensional concentrators and, therefore, an adaptation of the deduction for the bidimensional case can be made. The Bidimensional deduction of the mean square value of different probabilistic total error distribution, results in:

$$\sigma_{pb} \approx \frac{\theta_s}{\sqrt{3}} \qquad \text{(eq. 17)}$$

4. Thermal efficiency calculation

The thermal efficiency considers, in addition to optical efficiency, the influence the C. It is relevant because it allows to reduce the thermal losses in the proportion of 1/C, and can be calculated using the ratio of the absorber's area (A_{ab}) and the total aperture area of the concentrator (A_{abs}).

$$C = \frac{A_{ab}}{A_{abs}} \quad \text{(eq. 18)}$$

In the linear Fresnel concentrator, the energy collection aperture is based on all the extension of the field of primary mirrors, that is, the total area of the terrain, including spaces between the mirrors. Increasing the space between the primary mirrors, without altering their width, increases C, but also increases the ground losses, reducing the optical efficiency (Souza et al., 2021, 2023). Throughout the study, the concentration was calculated based on the coordinates at the edge of the last mirrors. Therefore, the aperture is the distance between the edges of the mirrors further away from the origin of the system (the absorber), as shown in Figure 2.

For linear concentrators and cylindrical absorber, the radius Rabs, with longitudinal length of the set of primary mirrors L. Before calculating the concentration through the aperture, all the mirrors have the same height and are juxtaposed, that is, positioned in with no space between them in the scenario in which their normal are perpendicular to the horizontal plane. In the real operation of the system, this scenario never happens, since all the mirrors have different inclination that varies with the positioning of the sun. So here is eq. 19.

$$C = \frac{\text{aperture}}{2\pi R_{abs}} \quad \text{(eq. 19)}$$

Using the equations of Fraidenraich et al. (1999) describing this relationship, the thermal efficiency (η_{th}) is eq. 20. With losses_{th} the thermal losses proportional to the temperature of the absorber measured in s W/m obtained by the characterization of the Schotty absorber tube (Burkholder and Kutscher, 2009), and the DNI is the direct normal incident over the aperture of the concentrator measured in W/m².

$$\eta_{th} = \eta_{opt} - \frac{\text{losses}_{th}}{\text{DNI} \times 2 \times \pi \times R_{abs} \times C} \quad \text{(eq. 20)}$$

Caution is need so that the benefit of thermal losses reduction through the increase of the concentration does not re-duce the intercept factor and, consequently, the optical efficiency in such magnitude that the thermal efficiency becomes lower.

5. Linear Fresnel reflector review

In the case of LFR, designs have been idealized with the goal of improving its optical performance in the systems with evacuated absorber tube, from the inclusion of secondary at a short distance above the glass tubes envelopes of the absorber. The secondary used in LFR can be divided in (a) Concentrators with predefined geometry, the majority being Compound Parabolic Concentrator (CPC), Compound Elliptical Concentrator (CEC), trapezoidal or two-wings or (b) Optimized concentrators (obtained tailored for the primary, or point to point, adaptively from a pre-existing primary.

Feuermann and Gordon (1991), first discussed the LFR idea with double reflection using a CPC-type secondary, obtaining a 67 % of optical efficiency, at a concentration of 18.2, with absorber at a 2.2 m height.

Canavarro et al. (2014) employed the Simultaneous Multiple Surface (SMS) method to obtain a tailored secondary, achieving a 70 % optical efficiency at a geometric concentration of 52.95, (for θ_s = 12 mrad) and a higher efficiency of 72% at C=73.71 (for θ_s= 7.7 mrad), illustrating the efficiency/concentration trade-off and the impact of solar profile width.

Qiu et al. (2017) explored the use of primary mirrors with curvature and two secondary types (trapezoidal and CPC), obtaining η_{opt} around 65% to 67%. Their simulations rigorously included both the sun's brightness (uniform, θ_s = 4.65 mrad) and optical errors σ_{tot}= 1 mrad, Gaussian).

Prasad et al. (2017) achieved the highest reported optical efficiency (η_{opt}= 76.4 %) using a Segmented Parabolic Concentrator (SPC) secondary combined with an individualized sight line for each cylindricallycurved primary mirror. However, including optical errors σ_{tot}= 4.4 mrad) reduced the performance significantly to less than 68 %. A simpler CPC design in their study maintained a good performance (η_{opt}= 76.4 %) with error inclusion, albeit with non-uniform flux distribution.

Hack et al. (2017) compared a secondary obtained via an adaptive optimization method against standard shapes (CPC, trapezoidal, two-wings), achieving η_{opt}= 72 % at C= 37.13 under a total Gaussian deviation of σ_{tot}= 7 mrad. Vouros et al. (2019) similarly optimized a CPC, reaching η_{opt}= 75% at at C= 27.5, but performance dropped below 70% when the total deviation increased to σ_{tot}=12 mrad.

Sánchez-González and Gómez-Hernández (2020) proposed a novel beam-down LFR system, achieving a very high geometric concentration C= 88.9, however, there is a low interception factor equal to 0.372 due to the complexity and height of the system (75).

Souza et al. (2023) presents superior designs of Linear Aplanatic Fresnel Reflector (LAFR). The equations for the two mirror shapes in the original aplanat have closed-form solutions that follow from satisfying both Fermat's principle of equal optical path length and the Abbe sine condition for all incident paraxial rays (Gordon, 2010). They eliminate the spherical and coma aberrations and are reported explicitly in (Gomes et al., 2019; Gordon, 2010) and, for the sake of brevity, will not be repeated here. The solutions require two input parameters, s and K, that relate the position of the vertices of the primary and secondary mirrors to each other and to the focus, respectively, both relative to the focal length of the Abbe sphere intrinsic to aplanatic design (Gordon, 2010). The performance and practical virtues of 2D dual-mirror aplanats as alternatives to PTCs were first elaborated in (Gomes et al., 2019). Ray trace simulations results using θ_s = 9 mrad and σ_{tot}= 4.5 mrad are available for this work and indicates that intercept factor of 0.89 can be reached for s = -2.25 and K = -0.03 at the geometric concentration C = 35.

The intercept factor presented in Table 1 was calculated dividing the optical efficiency by the optical properties of the concentrators, both available in the articles. The aspect ratio is the height of the secondary divided by the full primary aperture. About Errors σ_{tot} and Sun Width uses G for Gaussin and U for Uniform distribution.

Table 1: Table captions (8 pt) should be centered and placed above the table.

Authors	η_{opt} **(%)**	**C**	**Absorber/ Secondary set height**	**Aspe ct Ratio**	**ρτα**	γ	**Errors** σ_{tot} **(mrad)**	**Sun width** θ_s **(mrad)**
Souza et al. (2023)	78.3	35	8.3	1.06	0.88	0.89	4.5 G	9 G
Sánchez-González and Gómez-Hernández (2020)	37.2	88.9	75	0.007	1	0.37 2	-	4.69 U
Vouros et al. (2019)	75	27.5	2.57	0.502	0.93	0.81	7 G	-
Bellos et al. (2018)	72.84	20.46	-	0.5	0.82	0.89	-	4.65 U
Hack et al. (2017)	72	37.13	7	0.547	0.88	0.82	7 G	-
Canavarro et al. (2017)	70	45	10.8	0.415	0.86	0.81	-	13.1 U
Prasad et al. (2017)	75	58	7.9	0.449	0.83	0.90	4.4 G	-
Qiu et. al. (2017)	65.4	68	8	0.392	0.85	0.77	1 G	4.65 U
Canavarro et al. (2014)	70	52.95	9.8	0.487	0.84	0.83	-	12 U
Feuermann and Gordon (1991)	67	18.2	2.2	0.458	0.90	0.74	17.158 G	4.65 U

Studies show that it is not possible to make a comparison analyzing only the optical efficiency or concentration values. Different total error probabilistic distribution, transmissivity and reflectivity were used. The total error probabilistic distribution can be adapted for gaussian for every work analyzed using Eqs. 14-16. It is also noted a considerable difference between the geometric concentrations calculated, which can be analyzed along with optical efficiency, because they define the thermal efficiency (Bendt et al., 1979). The concentration reduces the thermal losses, but the effect of this reduction does not interfere significantly in the thermal efficiency when the losses term is little compared to the optical efficiency.

6. Results

The results are divided into two main components. First, to complete the Linear Aplanatic Fresnel Reflector (LAFR) design analysis presented by Souza et al. (2021, 2023), which was previously limited to presenting Incidence Angle Modifier (IAM) curves, Section 6.1 provides an unpublished estimation of the total annual solar energy absorbed by different LAFR projects, explicitly considering losses due to the secondary mirror's double-reflection. Following this, Section 6.2 applies the advanced analysis derived from the ten designs presented in this work. Using the mathematical equations from Sections 2, 3, and 4, we present the thermal efficiency curves as a function of the absorber tube temperature for each selected case.

6.1. Estimations of annual absorbed energy by linear aplanatic Fresnel reflectors

As the LAFR geometric and optical characteristics and the incidence angle modifiers for each one are available for this work, the parameters s and K of these concentrators were varied and the annual energy absorbed of different designs in the Petrolina city, Pernambuco, Brazil (9.1°S, 40.3°W) – which annual sum of the direct normal irradiance at the aperture plane of the concentrator is ~1.42MWh/m², considering the meteorological data of time series obtained from Solargis, software that offers solar and climate data for solar energy projects, with the following average values of reflectivity, absorptivity, and transmissivity: ρ=0.95, α=0.96 and τ=0.963.

The parameters s and K relates the position of the vertices of the primary and secondary mirrors to each other and to the focus, respectively (Gordon, 2010; Souza et al., 2021). The model for the estimation of energetic absorption is presented in the Eqs. 1-12. The intercept factor was calculated for all the designs through raytracing, considering Gaussian distribution with σ_{tot} = 4.5 mrad.

Table 2: Estimation of the total energy absorbed during one year by different linear aplanatic Fresnel reflectors, considering the time series obtained from SolarGis.

Annual total energy absorbed (MWh/m²)	Annual energy absorption efficiency	Parameters {s; K} that defined the LAFR	Interception factor in the normal incidence (θ = 0°)	Absorber height (m)	Aspect ratio	C
0.78	0.47	{-1; -0.1}	0.68	3.7	0.33	50.3
0.85	0.51	{-1; -0.03}	0.75	3.7	0.36	46.2
0.97	0.58	{-1.3; -0.1}	0.79	4.8	0.52	41.8
1.01	0.61	{-2.25; -0.03}	0.89	8.3	1.06	35

The consistently good thermal performance observed across all tested LAFRs is comparable to the best concentrators reported in the literature. Specifically, the LAFR {-2.25; -0.03} achieved a total annual efficiency of 0.61. This aplanatic concentrator is selected as the benchmark for comparisons in the next section.

In previous works Souza et al. (2021, 2023), θ modifiers are presented for two cases presented here, {s = -1; K = -0.1} and {s = -2.25; K = -0.03}. It is found that the height of the absorber directly interferes in the transversal and longitudinal incidence angle modifiers. Higher absorbers have better transversal interception factor, however, lower concentration. These advantages observed in the calculation of the amount of absorbed energy provide a higher energy collection and a higher efficiency of annual energy absorption.

The thermal efficiency curve for each case was obtained from Eq. 20, setting DNI = 800 W/m² and Rabs = 35 mm, function of the temperature of the absorber tube for the four concentrators with promising practical characteristics observed in Table 2, and considering normal incidence of the sun in the aperture of the concentrators. That is, it is instantaneous and calculated at solar noon. It was possible to evaluate a representative set of good LFARs with practical characteristics suitable for solar fields of CSP plants. The thermal losses of the Schott absorber tube were considered for all cases, and the optical properties were obtained individually from the articles analyzed. However, the larger thermal losses were considered, assuming that there are no physical obstacles around the absorber. The real losses should be lower and depend on the geometry of the secondary reflector and the distance between this and the absorber.

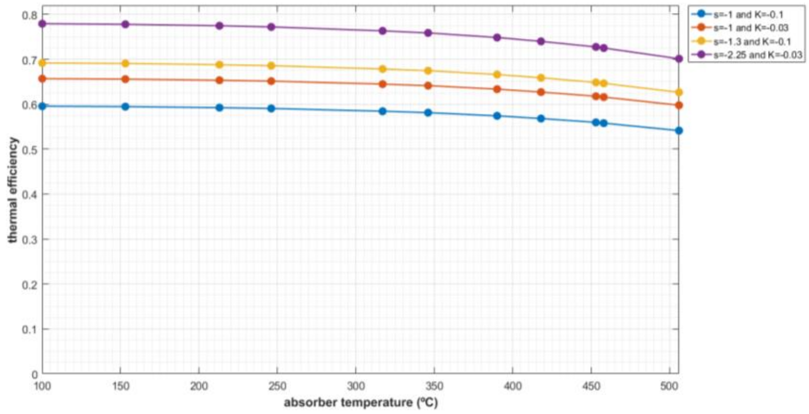

Figure 3. Thermal efficiency in function of temperature for different LAFR with thermal losses data from Schotty absorber tube, DNI = 800 W/m² and Rabs = 0.035 m.

The LAFR {-2.25; -0.03} has superior performance because it presents high interception factor (~0.9), maintaining high concentration (C=35). For comparison, parabolic troughs have a concentration of 26, for an intercept factor of ~0.9. For other concentrators, the increase of concentration observed results in significant reduction of optical efficiency, which negatively affects the thermal efficiency. Due to the best performance, was chosen for a broader evaluation, considering other optical projects, presented in Figure 4.

The model for estimating the annual absorbed energy, detailed in Equations 1 through 12, is inherently transferable to any geographical location. To broaden the research impact, it is only necessary to substitute the hourly time series of DNI and the local meteorological data (latitude, longitude, time of day, and day of the year for calculating the θ_t and θ_l) of Petrolina city with equivalent annual data from the new region of interest. This adaptation would allow calculating the E_{year} and the annual absorption efficiency for the same set of LAFR concentrators across different climatic and solar zones, thus amplifying the research's practical scope and impact on global CSP projects.

6.2. Thermal efficiency curves of the ten concentrators analyzed

Analogous to what was done in the result presented in Figure 3, and expanding the analysis, the result presented in Figure 4 considers the ten best concentrators identified in the literature – presented and discusses in Section 5 – which provide practical data of concentration and optical efficiency, allowing the thermal efficiency curve presented.

For this result, the information contained in the articles, such as presented, are used. This way, the loss by double-reflection on the secondary mirror is not estimated, where the optical efficiency of the final value calculation consid-ered and gathered from each publication.

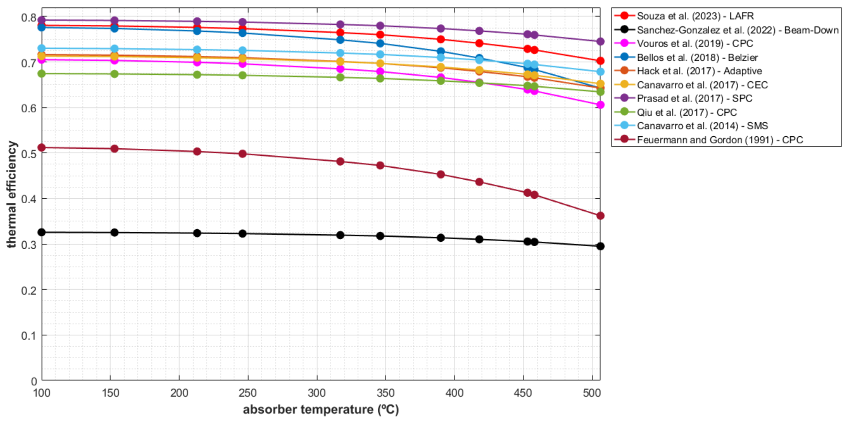

Figure 4. Comparison of the Thermal Efficiency in function of temperature for the Schotty absorber tubes between the LFR found in the literature. DNI = 800 W/m² and Rabs = 0.035 m.

It is important to acknowledge the limitations inherent in the comparative analysis presented in Figure 4. Firstly, the reliance on the final optical efficiency reported in the literature, without re-estimating factors such as the loss from double-reflection on the secondary mirror for all designs, introduces a slight comparative inconsistency. More crucially, the comparison is limited by the non-normalization of the diverse probabilistic total error distributions (σ_{tot}) across the ten concentrators, a key step discussed in Section 6.3. The absence of sufficient input data from the literature prevents this normalization, hindering a fully fair comparison and potentially leading to performance over- or under-estimations for some designs. Secondly, in calculating thermal efficiency, the model conservatively considers the largest thermal losses of the bare Schott absorber tube, assuming no surrounding physical obstacles or an optimized secondary reflector cavity. Consequently, the efficiency curves shown should be interpreted as a lower performance boundary; in an optimized engineering project, actual thermal losses are expected to be lower, resulting in higher real-world efficiencies.

Comparing with other practical studies of LFR and PTC plants, such as the one presented by Schenk et al., (2014), it is possible to observe the potential of the concentrators analyzed in this work to considerably surpass the performance of conventional systems in the analyzed temperature range. As observed throughout the results, conventional LFR systems without secondary have typical thermal efficiency of 0.65, decreasing when increasing temperature. In relation to the PTC, the thermal efficiency is in the order of 0.8, similar to the concentrators presented in this work. However, a sharp drop in the efficiency value is observed when the absorber temperature increases. This is not the case for LFR with secondary because they can achieve concentrations much higher than PTCs (typically limited to ~26), maintaining high optical efficiency.

Fixing an appropriated temperature value for the CSP plant operation with linear concentrators fields at 390°C, and removing the characterization of the Schotty tubes, which thermal losses for this temperature is 204 W/m, it is possible to draw a thermal efficiency curve in function of direct normal irradiance shown in Figure 5.

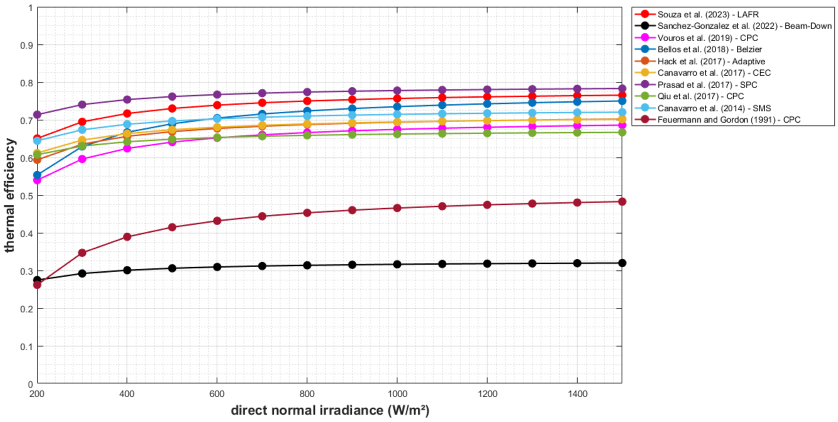

Figure 5. Thermal efficiency in function of the DNI for absorber temperature equal to 390°C and Rabs= 0.035m.

6.3. Sensitivity of the interception factor to the total error probabilistic distribution

The analysis of the concentrators should be improved considering a normalization of the total error distributions values. Thus, part of Table 1 can be modified, considering Eqs. 14-17, to obtain the equivalent Gaussian distributions for each case. This is not done here, cause the necessary information about the concentrators to calculate intercept factor or optical efficiency are not available.

The optical efficiency strongly depends on the mean squared value of the probabilistic distribution of total errors used in ray tracing simulations and should guide the evaluation and choice of this type of device for applications in CSP solar fields.

The results presented in Figures 4 and 5 may change significantly if the distributions are normalized for each case. It can be seen, for example, that the performance of the concentrator proposed by Prasad et al. (2017), which is at the top, may suffer a sharp drop in intercept factor, if a total deviation of errors equal to 7 mrad is used, much higher than that considered by the authors.

On the other hand, the projects presented by Vouros et al. (2019) and Hack et al. (2017) can have a substantial improvement if the mean of the total deviations observed is used, for example, which is 4.518 mrad, well below that used by the authors. It can also be seen that the concentrator presented by Feuermann and Gordon (1991) can reach a much higher interception factor value than the one presented if the mean of the total deviations observed in the articles is used instead of a high value of 17.158 mrad used by the authors.

7. Conclusion

In the present work, linear Fresnel concentrators with high optical and thermal performance were identified and analyzed. Some showed good performance, with an intercept factor ~0.9 and a concentration above 35, much higher than parabolic troughs, maintaining the inherent advantages to the linear Fresnel concentrators. It was observed in the vast literature available that LFR was conceived without secondary. Scientific findings over the years have determined that every LFR have primary segmented mirror that track the Sun in such manner as to concentrate energy in a linear focus and must to include a non-image forming secondary mirror to prevent losses by excessive dispersion.

Iterative numerical procedure generally is used to identify practical settings of high-performance solar concentrators and its optical performance. A central category of the optical design is adopted (for example, PTC or LFR, including secondary concentrators) and its geometric design parameters affect the optical gains. That way, the designs obtained from the variation of these associated parameters should be evaluated through numerical ray tracing simulations, which should consider millions of beams to become valid. The results are compared, considering the design decisions that can maximize the performance. Given this scenario, the LAFR is advantageous among the concentrators analyzed, for it has performance comparable to the best linear concentrators, having closed formulation, with dismiss iterative calculation and facilitates the concentrator's optimization.

The findings of this study provide a vital analytical tool for concentrating solar power (CSP) project engineers. The derived thermal efficiency curves (Figure 4) allow for the optimal selection of LFR geometry based on the required operating temperature and local DNI conditions, which is crucial for system optimization. The demonstrated performance of the LAFRs is particularly impactful: they achieve thermal efficiencies comparable to PTCs but at significantly higher concentration ratios (C>35). This high concentration is key to minimizing thermal losses per unit of aperture area, directly contributing to a reduction in the LCOE for CSP plants. Furthermore, the LAFR's non-iterative, closed analytical formulation offers a significant engineering advantage, facilitating rapid design assessments, preliminary design optimization, and potential integration into real time control systems.

As the average annual optical gains depend on climate and latitude, the LFR design optimization will always be specified for each case. However, some works present useful analytical tools to evaluate the optical and thermal performance of the LFR in any situation through the incidence angle modifier. The losses considered inherent to the transversal and longitudinal incidence angle variations need to be evaluated when the annual performance is calculated. In this work, this calculation was performed for a particular concentrator, the LAFR, being the LAFR with parameters s = -2.25 and K = -0.03 the best performance observed.

For determined conditions of operation temperature demanded in the field of collectors and the turbine, the vital evaluation to decide within the different designs is the optical and thermal efficiency of the solar concentration system, along with the practical matters of cost, installation, operation and maintenance. This work presented a methodology for calculating the thermal efficiency as a function of the temperature of the absorber tube and the instantaneous direct normal irradiance, which involves two important parameters of solar concentrator projects: intercept factor and geometric concentration. This way, the rest of the thermal solar plant (that is, the power block performance) is not approached here and is therefore delegated for future studies.

The analytical tools presented resulted in a range of possibilities of future optimization studies that will open other design and engineering possibilities for the development of LFR prototypes that help reducing leveled costs of CSP energy. The mean squared value of the total error distribution directly influences the intercept factor results. Thus, it is expected that concentrators that perform well for small σ_t values may have a lower intercept factor for larger values, and therefore lower optical efficiency. Using a high σ_t and obtaining a good result indicates an excellent performance of the concentrator, which is less susceptible to tracking errors, misalignment, and imperfections of the reflective surface.

Finally, the practical restrictions imposed to the designs analyzed here are common to conventional commercial LFR solar plants. There can be different or additional limitations for future customized systems, cases in which analytical derived approaches in the works examined will provide the designers with a direction for immediate analysis and quantification of any source of optical or thermal losses of decisive importance in the face of such restrictions.

8. References

Alami, A. H., Olabi, A. G., Mdallal, A., Rezk, A., Radwan, A., Rahman, S. M. A., Shah, S. K., Abdelkareem, M. A. (2023). Concentrating solar power (CSP) technologies: Status and analysis. International Journal of Thermofluids. v. 18, 100340.

Bellos, E., Tzivanidis, C. (2018). Development of analytical expressions for the incident angle modifiers of a linear Fresnel reflector. Sol. Energy, 173, 769–779.

Bellos, E., Tzivanidis, C., Papadopoulos, A. (2018). Secondary concentrator optimization of a linear Fresnel reflector using Bezier polynomial parametrization. Solar Energy, Elsevier, v. 171, p. 716-727.

Bendt, P., Rabl, A., Gaul, H. W., Reed, K. A. (1979). Optical Analysis and Optimization of Line Focus Solar Collector. Solar Energy Research Institute, Golden, CO, p. 76.

Biggs, F., Vittitoe, C. N. (1979). The Helios Model for the Optical Behavior of Reflecting Solar Concentrators. SAND 76-0347.

Burkholder, F., Kutscher, C. (2009). Heat Loss Testing of Schott's 2008 PTR70 Parabolic Trough Receiver. Technical Report NREL/TP-550-45633.

Canavarro, D., Chaves, J., Collares-Pereira, M. (2014). Simultaneous multiple surface method for linear Fresnel concentrators with tubular receiver. Solar Energy, Elsevier, v. 110, p. 105-116.

Canavarro, D., Chaves, J., Collares-Pereira, M. (2017). New dual asymmetric CEC linear Fresnel concentrator for evacuated tubular receivers. AIP Conf. Proc., p. 1850, 040001.

CSTA (2022). Blue Book of China’s Concentrating Solar Power Industry 2021. China Solar Thermal Alliance (CSTA), Beijing.

Chen, X., Wang, F., Yan, X., Cheng, Z., Han, Y., Jie, Z. (2018). Thermal and chemical analysis of methane dry reforming in a volumetric reactor under highly concentrated solar radiation. Solar Energy, Elsevier, v. 162, p. 187–195.

Feuermann, D., Gordon, J. M. (1991). Analysis of a two-stage linear fresnel reflector solar concentrator. Journal of Solar Energy Engineering, Transactions of the ASME, v. 113, n. 4, p. 272-279.

Fraidenraich, N., Lyra, F. (1995). Energia Solar: fundamentos e tecnologia de conversão heliotérmica e fotovoltaica. Ed. Universitária da UFPE, Recife, p. 56-67.

Fraidenraich, N., Lima, R. C. F., Tiba, C., Barbosa, E. M. S. (1999). Simulation model of a CPC collector with temperature dependent Heat loss coefficient. Solar Energy, Vol. 65, No. 2, pp. 99–110.

Gaul, H., Rabl, A. (1980). Incidence-Angle Modifier and Average Optical Efficiency of Parabolic Trough Collectors. ASME. J. Sol. Energy Eng., 102(1), 16–21.

Giostri, A., Binotti, M., Silva, P., Macchi, E., Manzolini, G. (2012). Comparison of Two Linear Collectors in Solar Thermal Plants: Parabolic Trough Versus Fresnel. Journal of Solar Energy Engineering, 135, 1-9.

Gomes, E. T. A., Fraidenraich, N., Vilela, O. C., Oliveira, C. A. A., Gordon, J. M. (2019). Aplanats and analytic modeling of their optical properties for linear solar concentrators with tubular receivers. Sol. Energy, 191, 697-706.

Gordon, J. M. (2010). Aplanatic optics for solar concentration. Optics Express, v. 18, p. A41-A52.

Gude, V. G. (2018). Use of exergy tools in renewable energy driven desalination systems. Thermal Sci. Eng.

Prog., Elsevier, v. 8, p. 154–170.

Hack, M., Zhu, G., Wendelin, T. (2017). Evaluation and comparison of an adaptive method technique for improved performance of linear Fresnel secondary designs. Applied Energy, 208, 1441-1451.

Howell, J.R., Mengüç, M.P., Siegel, R. (2016). Thermal radiation heat transfer. CRC Press, Boca Raton.

Hussain, M. I., Lee, G. H. (2016). Thermal performance comparison of line- and point-focus solar concentrating systems: Experimental and numerical analyses. Solar Energy, 133, 44-54.

Manikandan, G.K., Iniyan, S., Ranko, G. (2019). Enhancing the optical and thermal efficiency of a parabolic trough collector – a review. Appl. Energy, 235, 1524–1540.

McIntire, W.R. (1982). Factor approximations for biaxial incident angle modifiers. Sol. Energy, 29, 315-322.

Mishra, R. S., Singh, H. (2018). Detailed parametric analysis of solar driven supercritical CO2 based combined cycle for power generation, cooling and heating effect by vapor absorption refrigeration as a bottoming cycle. Thermal Sci. Eng. Prog., Elsevier, v. 8, p. 397–410.

Pettit, R. B., Vittitoe, C. N., Biggs, F. (1983). Simplified Calculational Procedure for Determining the Amount of Intercepted Sunlight in an Imaging Solar Concentrator. Journal of Solar Energy Engineering, v. 105, p. 101-107.

Prasad, G.S.C., Reddy, K.S., Sundararajan, T. (2017). Optimization of solar linear Fresnel reflector system with secondary concentrator for uniform flux distribution over absorber tube. Solar Energy.

Qiu, Y., Li, M. J., Wang, K., Liu, Z. Bin, & Xue, X. D. (2017). Aiming strategy optimization for uniform flux distribution in the receiver of a linear Fresnel solar reflector using a multi-objective genetic algorithm. Applied Energy.

Rabl, A. (1985). Active Solar Collectors and Their Applications. Oxford University Press, New York.

Sánchez-González, A., Gómez-Hernández, J. (2020). Beam-down linear Fresnel reflector: BDLFR. Renewable Energy, v. 146 pp. 802-815.

Santos, A. V., Canavarro, D., Horta, P., Collares-Pereira, M. (2021). An analytical method for the optical analysis of Linear Fresnel Reflectors with a flat receiver. Sol. Energy, 227, 203-216.

Schenk, H., Hirsch, T., Feldhoff, J. F., Wittmann, M. (2014). Energetic Comparison of Linear Fresnel and Parabolic Trough Collector Systems. ASME. J. Sol. Energy Eng., 136(4): 041015.

Souza, L. F. L., Fraidenraich, N., Tiba, C., Gordon, J. M. (2021). Linear aplanatic Fresnel reflector for practical high-performance solar concentration. Sol. Energy, 222, 259-268.

Souza, L. F. L., Paes, M. D. A., Tiba, C. (2021). Análise financeira da produção combinada de Eletricidade e calor de processo industrial com Energia solar. Revista Brasileira de Eneriga Solar, v. 12, n. 1, p. 87– 96.

Souza, L. F. L., Fraidenraich, N., Tiba, C., Gordon, J. M. (2023). Analytic optical evaluation of linear aplanatic solar Fresnel reflectors. Sol. Energy, 249, 107-121.

Vouros, A., Mathioulakis, E., Papanicolaou, E., Belessiotis, V. V. (2019). On the optimal shape of secondary reflectors for linear Fresnel Collectors. Renewable Energy, v. 143(C), p. 1454-1464.

Wang Y, Zhu Y, Chen H, Zhang X, Yang L, Liao C. (2015). Performance analyss of a novel sun-tracking CPC heat pipe evacuated tubular collector. Appl Therm Eng, v. 87, pp. 381–8.

Yao, L., Wang, Y., Xiao, X. (2024). Concentrated Solar Power Plant Modeling for Power System Studies. IEEE Transactions on Power Systems, vol. 39, no. 2, pp. 4252-4263.

Zhu, G. (2013). Development of an analytical optical method for linear Fresnel collectors. Sol. Energy, 94, 240-252.